Dry deposition of organic trace gases addresses a poorly quantified process in the atmosphere (*3*, *10*). We estimate a lower and upper bound for the annual deposition flux of gas phase oVOCs between 37 and 56% relative to the annual NMVOC emission flux on a carbon basis (table S4). It is conceivable that oVOC deposition fluxes to vegetation could increase as a consequence of acute or chronic exposure to high O_3 concentrations in polluted regions (*16*).

References and Notes

1. A. H. Goldstein, I. Galbally, *Environ. Sci. Technol.* **41**, 1515 (2007).
2. A. Guenther *et al.*, *Atmos. Chem. Phys.* **6**, 3181 (2006).
3. M. Hallquist *et al.*, *Atmos. Chem. Phys.* **9**, 5155 (2009).
4. R. Atkinson, J. Arey, *Chem. Rev.* **103**, 4605 (2003).
5. F. Paulot *et al.*, *Science* **325**, 730 (2009).
6. J. Lelieveld *et al.*, *Nature* **452**, 737 (2008).
7. W. J. Collins, R. G. Derwent, C. E. Johnson, D. S. Stevenson, *Clim. Change* **52**, 453 (2004).
8. C. A. Paulson *et al.*, *J. Appl. Meteorol.* **9**, 857 (1970).
9. M. L. Wesely, *Atmos. Environ.* **23**, 1293 (1989).
10. L. Zhang *et al.*, *Atmos. Environ.* **36**, 537 (2002).
11. R. Fall, *Chem. Rev.* **103**, 4941 (2003).
12. H. H. Kirch, D. Bartels, Y. Wei, P. S. Schnable, A. J. Wood, *Trends Plant Sci.* **9**, 371 (2004).
13. L. K. Emmons *et al.*, *Geosci. Model Dev.* **3**, 43 (2010).
14. Materials and methods are available as supporting material on *Science* Online
15. J. L. Jimenez *et al.*, *Science* **326**, 1525 (2010).
16. K. L. Denman *et al.*, in IPCC 4th Assessment Report, S. Solomon *et al.*, Eds. (Cambridge Univ. Press, Cambridge, 2007), chap. 7.
17. The National Center for Atmospheric Research is operated by the University Corporation for Atmospheric Research under sponsorship from the National Science Foundation.

Supporting Online Material

www.sciencemag.org/cgi/content/full/science.1192534/DC1
Materials and Methods
Figs. S1 to S16
Tables S1 to S4
References

19 May 2010; accepted 6 October 2010
Published online 21 October 2010;
10.1126/science.1192534
Include this information when citing this paper.

Transient Middle Eocene Atmospheric CO_2 and Temperature Variations

Peter K. Bijl,[1]*† Alexander J. P. Houben,[1]*† Stefan Schouten,[2] Steven M. Bohaty,[3] Appy Sluijs,[1] Gert-Jan Reichart,[4] Jaap S. Sinninghe Damsté,[2,4] Henk Brinkhuis[1]

The long-term warmth of the Eocene (~56 to 34 million years ago) is commonly associated with elevated partial pressure of atmospheric carbon dioxide (pCO_2). However, a direct relationship between the two has not been established for short-term climate perturbations. We reconstructed changes in both pCO_2 and temperature over an episode of transient global warming called the Middle Eocene Climatic Optimum (MECO; ~40 million years ago). Organic molecular paleothermometry indicates a warming of southwest Pacific sea surface temperatures (SSTs) by 3° to 6°C. Reconstructions of pCO_2 indicate a concomitant increase by a factor of 2 to 3. The marked consistency between SST and pCO_2 trends during the MECO suggests that elevated pCO_2 played a major role in global warming during the MECO.

The Middle Eocene Climatic Optimum [MECO; ~40 million years ago (Ma)] (*1*) interrupts a long-term middle Eocene cooling trend (*2*), with a globally uniform 4° to 6°C warming of both surface and deep oceans within ~400,000 years, as derived from foraminiferal stable oxygen isotope records (*3*). A decrease in carbonate mass accumulation rates during the MECO argues for ocean acidification induced by a rise in pCO_2 (*3*). Application of paleo-pCO_2 proxies across the MECO has yet to confirm whether pCO_2 changes are indeed associated with this interval of transient warming.

We investigated a sedimentary succession spanning the MECO recovered from the East Tasman Plateau at Ocean Drilling Program (ODP) Site 1172, which at that time was situated on the shelf (~65°S paleolatitude; Fig. 1 and figs. S1 and S2) (*4*, *5*). To fully capture the magnitude of the sea surface temperature (SST) change associated with the MECO at this site, we applied two independent temperature proxies: the alkenone unsaturation index ($U^{K'}_{37}$) (*6*) and the index of tetraethers consisting of 86 carbon atoms (TEX_{86}) (*5*, *7*) (fig. S3). At the onset of the MECO, $U^{K'}_{37}$ and TEX_{86} indicate a rise in SST of 3°C and 6°C, respectively, which, also at this location, stands out as an interruption of long-term middle Eocene cooling (Fig. 2). Bulk carbonate oxygen isotope values ($\delta^{18}O$) decrease by 1.0 to 1.2 per mil (‰), which, if controlled by SST only, also indicate a SST rise of ~4° to 5°C (*5*).

Additional evidence of warming is derived from assemblages of hypnozygotic organic cysts of surface-dwelling dinoflagellates (dinocysts) (*5*). Whereas the middle Eocene dinocyst record at ODP Site 1172 is dominated by taxa that are endemic to the Southern Ocean (*8*), an incursion of low-latitude dinocyst taxa characterizes the MECO (Fig. 2 and fig. S4). A SST increase of 3° to 6°C is consistent with inferences from benthic foraminiferal and fine-fraction carbonate oxygen isotope records at other sites (*1*, *3*). The $U^{K'}_{37}$ and TEX_{86} proxies are independent of seawater $\delta^{18}O$. Hence, the consistent magnitude of warming between the proxies suggests that the carbonate $\delta^{18}O$ records were not affected by a change in $\delta^{18}O$ of seawater, and that global ice volume did not change considerably during the MECO.

Absolute SSTs as indicated by $U^{K'}_{37}$ and TEX_{86} are consistent, with 26°C or 24°C just below the onset of the MECO for the two proxies, respectively, and peak MECO SSTs exceeding 28°C. These SSTs are much (~10°C) higher than those derived from fine-fraction carbonate oxygen isotope measurements from elsewhere in the Southern Ocean (*1*, *3*). At least part of this large discrepancy is most likely the result of diagenetic alteration of calcite (*9*).

We assessed pCO_2 changes by determining the stable carbon isotopic composition ($\delta^{13}C$) of alkenones, long-chained ketones exclusively synthesized by specific haptophyte algae. Carbon isotopic fractionation during carbon fixation (ε_p) by haptophyte algae varies as a function of dissolved CO_2 [$CO_{2(aq)}$] (*10*, *11*), specific cell physiological parameters (which show good correspondence to the surface-water concentrations of soluble phosphate), and other environmental parameters, primarily light intensity (*5*). The carbon isotopic composition of diunsaturated alkenones ($\delta^{13}C_{C37:2}$) ranges between –32.5 and –35.5‰ (fig. S3). We used bulk carbonate $\delta^{13}C$ to estimate the $\delta^{13}C$ value of the dissolved inorganic carbon (DIC) pool in seawater (*5*) to determine ε_p. The data show background ε_p values of 21 to 22‰ rising up to 24.5‰ during MECO (Figs. 2 and 3 and fig. S3). The relationship between ε_p and pCO_2 is exponential, which results in a relatively large uncertainty in reconstructed pCO_2 levels with high ε_p values (Fig. 3). Temperature variations, however, play a minor role in the range of temperatures indicated by TEX_{86} and $U^{K'}_{37}$ (Fig. 2) and cannot explain the high ε_p values (Fig. 3). It seems unlikely that changes in light intensity (*12*) influenced ε_p substantially at ODP Site 1172 (*5*). The soluble phosphate concentration exerts a strong influence on the relation between ε_p and pCO_2, particularly if ε_p values are high (*5*).

To evaluate all possible absolute pCO_2 estimates from our record, we applied the full range of present-day surface-water phosphate concentrations. These vary between 0 μmol liter^{-1} in the oligotrophic gyres to >2 μmol liter^{-1} in the Southern Ocean (*5*) (fig. S5). Yet even when phosphate concentrations of 0 μmol liter^{-1} are assumed, ε_p values between 21.2‰ and 24.5‰ yield pCO_2 estimates between 600 parts per million by volume (ppmv) before the MECO and 6400 ppmv during the MECO (Figs. 2 and 3). Hence, elevated levels of pCO_2 must in part be responsible for the high ε_p values, with middle Eocene pCO_2

[1]Biomarine Sciences, Institute of Environmental Biology, Faculty of Science, Laboratory of Palaeobotany and Palynology, Utrecht University, Budapestlaan 4, 3584 CD Utrecht, Netherlands. [2]Department of Marine Organic Biogeochemistry, NIOZ Royal Netherlands Institute of Sea Research, Post Office Box 59, 1790 AB Den Burg, Texel, Netherlands. [3]School of Ocean and Earth Science, University of Southampton, National Oceanography Centre, European Way, Southampton SO14 3ZH, UK. [4]Geochemistry, Department of Earth Sciences, Faculty of Geosciences, Utrecht University, Budapestlaan 4, 3584 CD Utrecht, Netherlands.

*These authors contributed equally to this work.
†To whom correspondence should be addressed. E-mail: p.k.bijl@uu.nl (P.K.B.); a.j.p.houben@uu.nl (A.J.P.H.)

being more than twice the pre-industrial value. When we assume maximal phosphate concentrations of 2 μmol liter^{-1}, pCO_2 ranges between ~2500 and ~24,000 ppmv (Figs. 2 and 3). The marginal marine Eocene East Tasman Plateau (*4*) likely experienced phosphate concentrations that were higher than 0 μmol liter^{-1} but lower than 2 μmol liter^{-1}, because closed oceanic gateways during the Eocene (*13*) prevented mixing associated with the Antarctic Circumpolar Current (ACC) that causes high phosphate levels in the present-day Southern Ocean. Eocene southwest Pacific surface-water phosphate concentrations were unlikely to have exceeded 1 μmol liter^{-1}, which implies maximum pCO_2 estimates of 1600 ppmv just before the MECO and 15,000 ppmv during the MECO (Figs. 2 and 3). With a realistic range of phosphate concentrations, pCO_2 values were between 600 and 1600 ppmv just before the MECO, which is in line with previous estimates of middle Eocene pCO_2 values using the same proxy (*14*), and rose to between 6400 and 15,000 ppmv during the MECO (Fig. 2, light gray band). MECO values exceed any previous Eocene alkenone-based estimate even when we assume phosphate concentrations of 0 μmol liter^{-1} (*5*). Despite uncertainties regarding absolute pCO_2 values, we note that the trends in pCO_2 follow those in the SST records remarkably well (Fig. 2).

Surface-water phosphate concentrations, however, may have varied in a marginal marine setting at ODP Site 1172. A tool for the reconstruction of phosphate concentration uses the remains of dinoflagellates (dinocysts), which are known to be

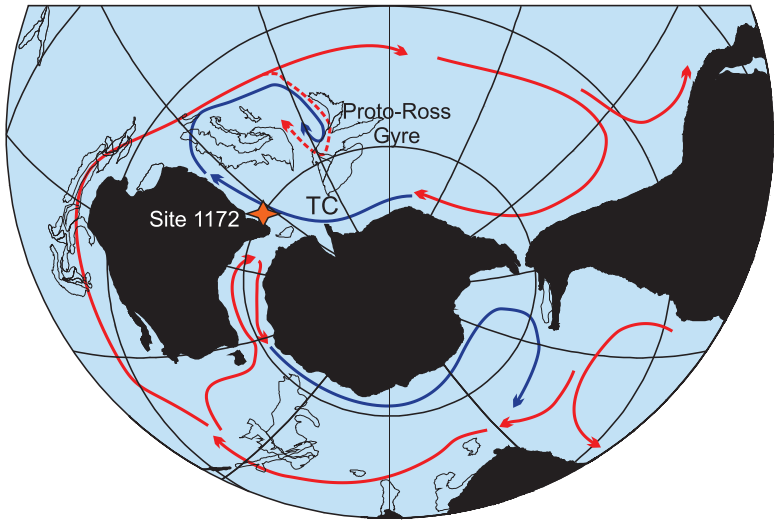

Fig. 1. Paleogeographic configuration of the southern high latitudes during the middle Eocene (~49 to 37 Ma; map was obtained from www.odsn.de) and ocean surface current configurations inferred from general circulation model experiments (*13*). The orange star indicates the paleogeographic location of ODP Site 1172 at 65°S in the southwest Pacific Ocean (*24*), under the influence of the Antarctic-derived Tasman Current (TC).

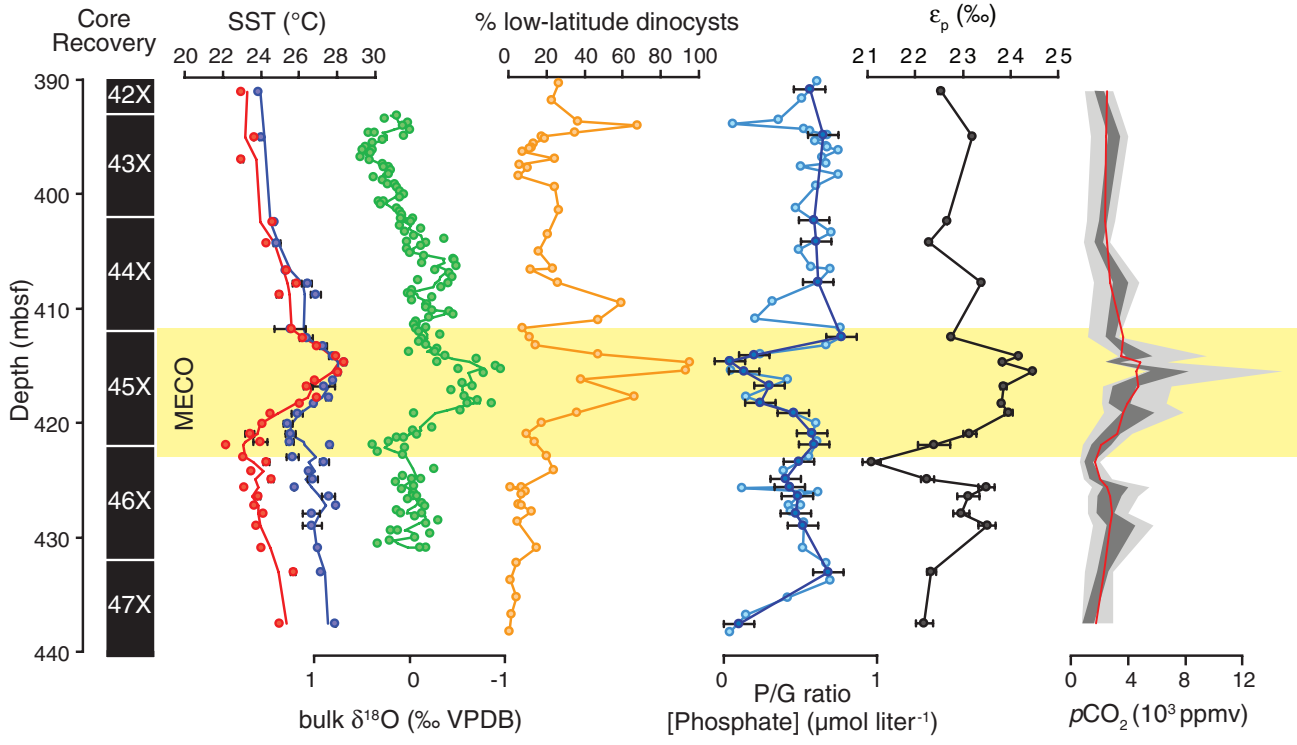

Fig. 2. Geochemical and palynological results across the MECO at ODP Site 1172, Hole A, cores 42X to 47X. The MECO is identified by integrating magnetostratigraphy (*25*), biostratigraphy (*25*), and chemostratigraphy (*3*) (see fig. S2). The $U^{K'}_{37}$ (purple), TEX_{86} (red), and bulk $\delta^{18}O$ (green) SST reconstructions show a warming of 3° to 6°C. The yellow shaded area delimits the MECO interval. The increase in percentage of low-latitude dinocysts (in orange) at the expense of endemic dinocysts during the MECO illustrates biotic response to warming. We estimated pCO_2 from carbon isotopic fractionation during carbon fixation (ε_p; black) by haptophyte algae with phosphate concentrations between 0 and 1 μmol liter^{-1} (light gray band). We further constrained phosphate estimates (dark blue line) by allowing phosphate concentrations to vary between 0.1 ± 0.1 μm liter^{-1} and 0.9 ± 0.1 μm liter^{-1} as a function of the ratio of peridinioid over gonyaulacoid dinocysts (P/G ratio; light blue line). This results in further constrained pCO_2 estimates (dark gray band). TEX_{86}, $U^{K'}_{37}$, oxygen isotope, and pCO_2 data are plotted with a 3-point running mean (solid orange, purple, green, and red lines, respectively). The error bars on TEX_{86} and $U^{K'}_{37}$ represent analytical error. On ε_p the error bars represent the difference between the use of TEX_{86} and $U^{K'}_{37}$ to determine ε_p.

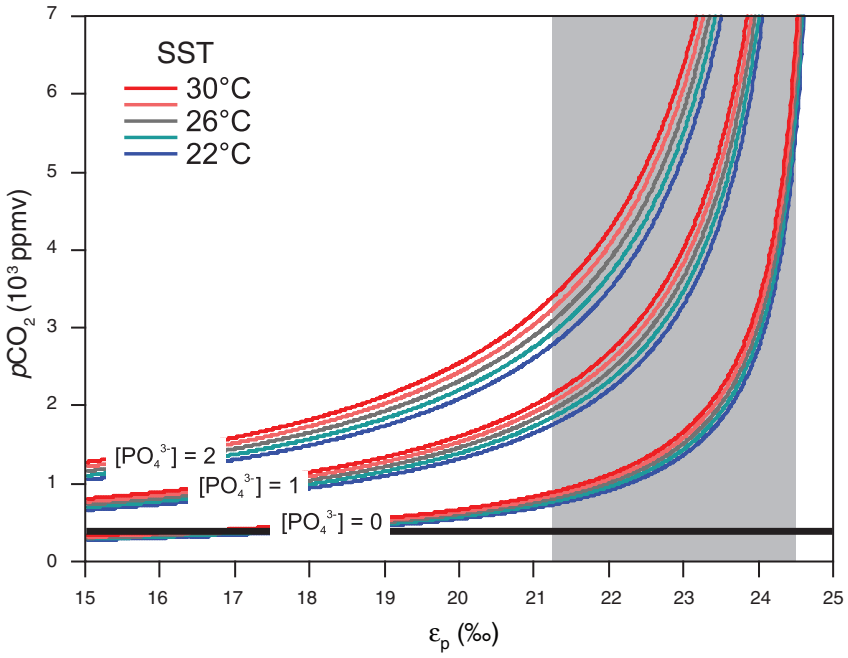

Fig. 3. Relationship between ε_p [versus VPDB (Vienna pee dee belemnite) standard] and pCO_2. The phosphate concentration ranges plotted are those from the present-day surface ocean, and the SST ranges (22° to 30°C) are those inferred from TEX_{86} and $U^{K'}_{37}$ data presented in Fig. 2 and a suite of Southern Ocean sites (*22*, *26*–*28*). The gray vertical bar indicates the values for ε_p as reconstructed for the MECO interval at ODP Site 1172, with use of TEX_{86}-based and $U^{K'}_{37}$-based SST reconstructions for these same levels, and bulk carbonate $\delta^{13}C$ measurements on the same section. Black horizontal line represents present-day pCO_2. Figure is modified from Pagani *et al*. (*10*).

extremely sensitive to surface-water nutrient availability changes (*5*). The ratio between peridinioid and gonyaulacoid dinocyst groups (the P/G ratio) is often used to reconstruct changes in relative nutrient abundance (*15*). The MECO at ODP Site 1172 shows a major decrease in the P/G ratio (*16*) (Fig. 2), suggesting a decrease in nutrient concentrations (*16*). As an experiment, we allowed phosphate to linearly vary as a function of the P/G ratio (Fig. 2) (*5*). The most prominent shift toward low P/G ratios occurs at MECO warming, resulting in lower phosphate concentration estimates. Also, when this drop in phosphate is taken into account, pCO_2 rises during the MECO and follows the SST trends (Fig. 2, dark gray band). Hence, regardless of the constraints on phosphate concentrations and other environmental parameters, pCO_2 levels must have been substantially higher during the MECO relative to the middle Eocene background.

One outstanding issue is the source of carbon responsible for the increase in middle Eocene atmospheric CO_2. The rise in pCO_2 by 2000 to 3000 ppmv emerging from our data requires a carbon source capable of injecting vast amounts of carbon into the atmosphere. Moreover, the absence of a prominent negative carbon isotope excursion excludes reservoirs with $\delta^{13}C$ signatures below that of marine DIC (*3*). One mechanism capable of emanating carbon with such a geochemical signature is the metamorphic alteration of carbonates (decarbonation) (*1*). Massive decarbonation occurred until the late Eocene, with the subduction of vast amounts of Tethyan Ocean pelagic carbonates under Asia as India drifted northward (*17*–*19*). However, the flux of carbon required to increase pCO_2 by 2000 to 3000 ppmv within ~400,000 years appears too high to invoke metamorphic (volcanic) outgassing as the sole mechanism.

Our pCO_2 and SST reconstructions allow for a tentative assessment of high-latitude climate sensitivity to CO_2 forcing on ~100,000-year time scales, assuming that all MECO warming was caused by pCO_2 and associated feedbacks. With an average 5°C SST increase and a factor of 2 to 3 increase in pCO_2, we arrive at a climate sensitivity of ~2° to 5°C per pCO_2 doubling. When we consider the pCO_2 decline from the Middle Eocene (~2000 ppmv; this study) to the latest Eocene (~1000 ppmv) (*20*) and the coeval high-latitude temperature decline (~3.5°C) (*21*, *22*), we derive similar values. Thus, long-term climate sensitivity to pCO_2 forcing in a world without the amplifying effects of ice-albedo feedbacks (*23*) may have been larger than previously anticipated.

References and Notes

1. S. M. Bohaty, J. C. Zachos, *Geology* **31**, 1017 (2003).
2. J. Zachos, M. Pagani, L. Sloan, E. Thomas, K. Billups, *Science* **292**, 686 (2001).
3. S. M. Bohaty, J. C. Zachos, F. Florindo, M. L. Delaney, *Paleoceanography* **24**, PA2207 (2009).
4. N. F. Exon, J. P. Kennett, M. J. Malone, Eds., *Proceedings of the Ocean Drilling Program, Scientific Results* (U.S. Government Printing Office, College Station, TX, 2003), vol. 189.
5. See supporting material on *Science* Online.
6. S. C. Brassell, G. Eglinton, I. T. Marlowe, U. Pflaumann, M. Sarnthein, *Nature* **320**, 129 (1986).
7. S. Schouten, E. C. Hopmans, E. Schefuß, J. S. Sinninghe Damsté, *Earth Planet. Sci. Lett.* **204**, 265 (2002).
8. H. Brinkhuis, S. Sengers, A. Sluijs, J. Warnaar, G. L. Williams, in *Proceedings of the Ocean Drilling Program, Scientific Results,* N. F. Exon, J. P. Kennett, M. J. Malone, Eds. (U.S. Government Printing Office, College Station, TX, 2003), vol. 189, pp. 1–48.
9. P. N. Pearson *et al*., *Nature* **413**, 481 (2001).
10. M. Pagani, *Philos. Trans. R. Soc. London Ser. A* **360**, 609 (2002).
11. Surface ocean CO_2(aq) originates from atmospheric CO_2 and deep waters, of which the latter is of major importance in marginal marine upwelling areas. Changes in upwelling through time may substantially change CO_2(aq) and hence would skew the reconstructed pCO_2 record. At Site 1172 we argue that a change in upwelling is not responsible for the signal we recorded in the alkenones, because that would have led to prominent shifts in the bulk carbonate carbon isotope profile (figs. S2 and S3).
12. B. Rost, I. Zondervan, U. Riebesell, *Limnol. Oceanogr.* **47**, 120 (2002).
13. M. Huber *et al*., *Paleoceanography* **19**, PA4026 (2004).
14. M. Pagani, J. C. Zachos, K. H. Freeman, B. Tipple, S. Bohaty, *Science* **309**, 600 (2005); 10.1126/science.1110063.
15. A. Sluijs, J. Pross, H. Brinkhuis, *Earth Sci. Rev.* **68**, 281 (2005).
16. U. Röhl *et al*., *Geophys. Monogr.* **151**, 127 (2004).
17. D. V. Kent, G. Muttoni, *Proc. Natl. Acad. Sci. U.S.A.* **105**, 16065 (2008).
18. J. C. Aitchison, J. R. Ali, A. M. Davis, *J. Geohys. Res.* **112**, B05423 (2007).
19. G. Dupont-Nivet, C. Hoorn, M. Konert, *Geology* **36**, 987 (2008).
20. P. N. Pearson, G. L. Foster, B. S. Wade, *Nature* **461**, 1110 (2009).
21. J. C. Zachos, G. R. Dickens, R. E. Zeebe, *Nature* **451**, 279 (2008).
22. Z. Liu *et al*., *Science* **323**, 1187 (2009).
23. M. Pagani, Z. Liu, J. LaRiviere, A. C. Ravelo, *Nat. Geosci.* **3**, 27 (2010).
24. N. Exon, J. P. Kennett, M. Malone, *Geophys. Monogr.* **151**, 367 (2004).
25. C. E. Stickley *et al*., in *Proceedings of the Ocean Drilling Program, Scientific Results*, N. F. Exon, J. P. Kennett, M. J. Malone, Eds. (U.S. Government Printing Office, College Station, TX, 2003), vol. 189, pp. 1–57.
26. C. E. Burgess *et al*., *Geology* **36**, 651 (2008).
27. C. J. Hollis *et al*., *Geology* **37**, 99 (2009).
28. P. K. Bijl *et al*., *Nature* **461**, 776 (2009).

29. This research used samples and data provided by the Ocean Drilling Program (ODP) sponsored by NSF and participating countries under the management of Joint Oceanographic Institutions Inc. We thank Utrecht University and the LPP foundation (P.K.B.), Statoil (A.J.P.H.), and the Netherlands Organization for Scientific Research (Vici grant to S.S.; Veni grant 863.07.001 to A.S.) for financial support. A.S. acknowledges the European Research Council under the European Community's Seventh Framework Program for ERC Starting Grant 259627. Groundwork for this research was provided at the Urbino Summer School of Paleoclimatology. We thank N. Welters, J. van Tongeren, J. Ossebaar, E. Hopmans, M. Kienhuis, G. Nobbe, E. van Bentum, E. Speelman, and E. van Soelen for technical support and M. Pagani, C. Stickley, J. Zachos, and two anonymous reviewers for invaluable discussions and comments.

Supporting Online Material

www.sciencemag.org/cgi/content/full/330/6005/819/DC1
Materials and Methods
SOM Text
Figs. S1 to S5
Tables S1 to S3

11 June 2010; accepted 17 September 2010
10.1126/science.1193654

Transient Middle Eocene Atmospheric CO_2 and Temperature Variations

Peter K. Bijl, Alexander J. P. Houben, Stefan Schouten, Steven M. Bohaty, Appy Sluijs, Gert-Jan Reichart, Jaap S. Sinninghe Damsté and Henk Brinkhuis

Science **330** (6005), 819-821.
DOI: 10.1126/science.1193654

The Dependable Warmer

During the middle of the Eocene, about 40 million years ago, a transient warming event interrupted the long-term cooling trend that had been in progress for the previous 10 million years. **Bijl *et al.*** (p. 819; see the Perspective by **Pearson**) constructed records of sea surface temperature and atmospheric CO_2 concentrations across the warming period. It appears that vast amounts of CO_2 were injected into the atmosphere, and a sea surface temperature increase of as much a 6°C accompanied the atmospheric CO_2 rise.